MEASUREMENTS AND CALCULATIONS OF THE LEAKAGE MULTIPLICATION FROM HOLLOW BERYLLIUM SPHERES

Calvin Wong, E. F. Plechaty, R. W. Bauer,
R. C. Haight, L. F. Hansen, R. J. Howerton,
T. T. Komoto, J. D. Lee, S. T. Perkins
and B. A. Pohl

Lawrence Livermore National Laboratory
University of California
Livermore, CA 94550

April 1985

Lawrence
Livermore
National
Laboratory

DISCLAIMER

MEASUREMENTS AND CALCULATIONS OF THE LEAKAGE MULTIPLICATION

FROM HOLLOW BERYLLIUM SPHERES*

Calvin Wong, E. F. Plechaty, R. W. Bauer, R. C. Haight, L. F. Hansen, R. J. Howerton,
T. T. Komoto, J. D. Lee, S. T. Perkins and B. A Pohl, Lawrence Livermore National Laboratory
P.O. Box 808
Livermore, CA 94550
(415) 422-4511

ABSTRACT

Using the Pulsed-Sphere Method, the leakage spectra from hollow Be spheres of 4.5, 13.8 and 19.9 cm thickness have been measured. The predicted copious production of epithermal and thermal neutrons from the 13.8 and 19.9 cm spherical shells has been verified. A quantitative comparison of measured and calculated time-of-arrival count spectra over the energy range from thermal to ∿ 15 MeV indicates that the ENDL-84 library overestimates the leakage spectra between 2 and 10 MeV and in the epithermal and thermal energy regions. In the remaining regions, the leakage spectra are underestimated. Because of the above compensation the inferred leakage multiplication for the 19.9 cm Be is ∿ 3% higher than calculations. In the case of the 13.8 cm Be, the compensation is less exact and the inferred leakage multiplication is ∿ 9% higher than calculations.

INTRODUCTION

Proposed fusion reactors [1,2] utilize Be in the surrounding blanket to multiply the fusion neutrons for use in breeding tritium and in some cases fissile materials. To have confidence that the breeding is correctly calculated, it is essential that the Be cross sections used have been validated via integral experiments. Recent measurements of the leakage multiplication from Be[3,4,5,6] and BeO [7] were 20 to 30% lower than calculations: Ref. (3) utilized Be cross sections evaluated by S. T. Perkins in 1968 [8]; Refs. (4,5,7) used ENDF/B-III cross sections; Ref. (6) utilized ENDF/B-IV. The leakage multiplication is defined as the number of neutrons leaking out of the Be per 14-MeV source neutron introduced at its center. Unpublished calculations of the leakage multiplication by Plechaty utilizing ENDL-80 (9) and ENDL-84 (10) were also approximately 25% higher than the above measurements.

In view of the large discrepancies observed irrespective of the libraries employed, we have undertaken a program to calculate and measure the leakage multiplication from spherical Be shells which were originally fabricated for criticality measurements on Be reflected assemblies. These shells have been assembled into thicknesses of 4.5, 13.8[a] and 19.9[a] cms. In all cases, the inner void radius was 8 cm. These Be thicknesses correspond to 0.8, 2.5, and 3.6 mean-free-path (MFP) for 14.8 MeV neutrons. An additional incentive for these measurements is to verify quantitatively the predicted copious emission of thermal and epithermal neutrons from the 2.5 and 3.5 MFP Be shells.

EXPERIMENTAL METHOD

The method utilized is that of "Pulsed Spheres" (11). The Be spherical shells are pulsed at their centers with nominal 14-MeV neutrons and neutrons leaving the spherical shells are measured by time-of-flight techniques at 7.28 meters with NE213, Stilbene, and ^{6}Li glass scintillators. Fig. 1 is a schematic diagram of the experimental geometry for the low energy spectra measurements with the 5.1 cm diameter by 1.9 cm thick ^{6}Li glass scintillator (11). The He bags reduce the attenuation of the epithermal and thermal neutrons. The space between the He bags is for the purpose of inserting absorbers such as ^{6}LiD, Cd or Au. The neutron production is monitored by counting the associated alpha particles with a silicon surface barrier detector at 165° to

---

[a]The 13.8 and 19.9 cm assemblies did not have a uniform thickness due to missing hemispherical shells (between $12.6 \leq r \leq 20.1$ cm) at the backward direction. The thicknesses in the backward hemisphere (towards the deuteron beam direction) are 6.3 and 12.4 cms, respectively.
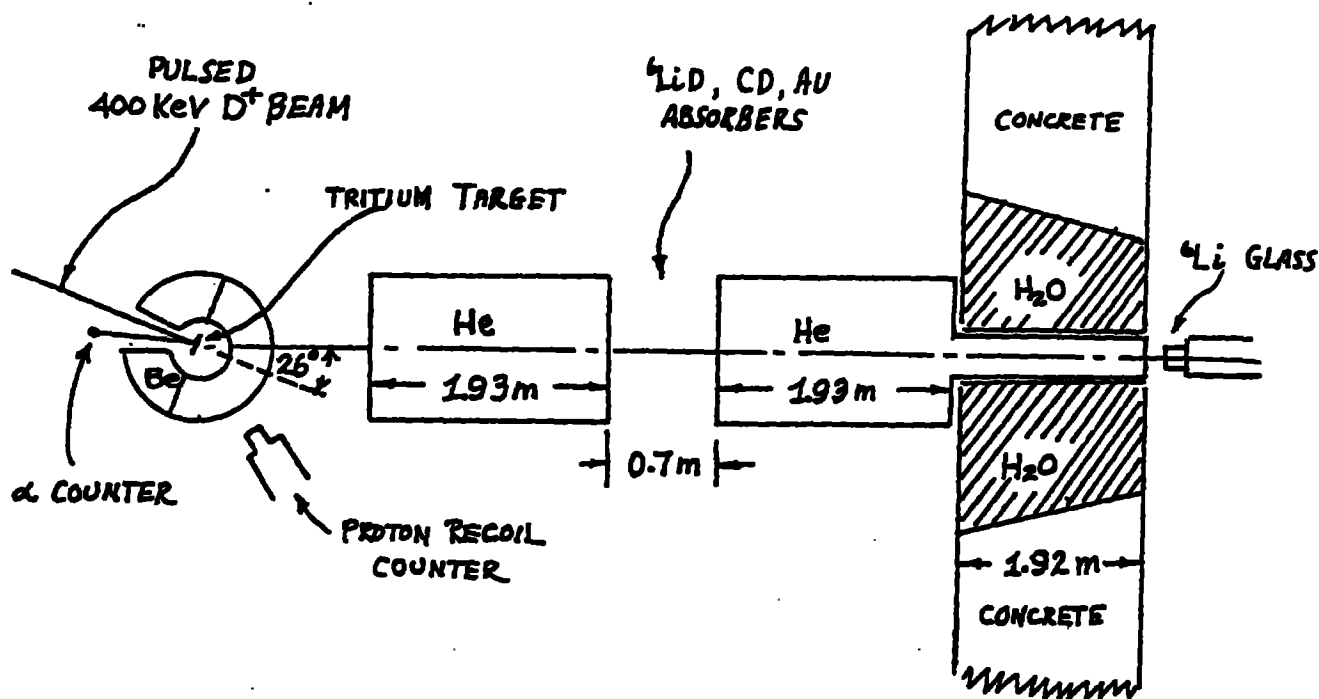
Fig. 1. Schematic Diagram (elevation, not to scale) of the experimental geometry for the low energy neutron spectra measurements.

the deuteron beam. With the Be removed, a proton recoil counter of known efficiency (12) at 50 cm was used to provide an absolute source strength calibration of the alpha counter. The proton recoil counter was left in place and periodic measurements of the alpha and proton recoil counts were made to check on the stability of the alpha counter. The ratio of proton recoil to alpha counts with the Be removed was constant within counting statistics, thereby attesting to the stability of the alpha counter as an absolute flux monitor. For the low energy measurements the pulsing frequencies and burst widths were: 100 Hz and 8 µs, and 1.667 kHz and 250 ns. For the high energy spectra measurements with Stilbene and NE213 detectors the pulsing frequency and burst width were 500 kHz and 2 ns, and the He bags were removed.

DETECTOR EFFICIENCIES

The Stilbene and NE213 detector efficiencies were determined by making pulsed-sphere measurements on a CH_2 sphere and requiring that the calculated time-of-arrival count spectra agree with the measured spectra. The rationale behind this method is that the hydrogen and carbon cross sections are well known and hence that the high energy emission spectra can be accurately

calculated. Since the high energy measurements are expressed as counts/ns per source count with the CH_2 sphere removed (essentially an attenuation measurement), a fit to the CH_2 data yields only a relative shape measurement of the efficiency versus energy. This is made absolute by determining the efficiency at 14.8 MeV by comparing the Stilbene and NE213 against the proton recoil counter whose efficiency is accurately known (12). These absolute efficiencies for NE213 at ∿ 3 and ∿ 1 MeV biases as determined above are shown in Fig. 2 as triangles and crosses, respectively. Also shown are efficiencies calculated with a computer code from G. Dietze and H. Klein (13). Good agreement is obtained between calculated and measured efficiencies. Comparable shape agreement was obtained with the Stilbene detector.

For the ^6Li glass detector, the efficiency was measured at the LLNL Electron Linac using a white neutron source with the ^6Li glass at 66 meters and a small ^{235}U fission chamber of known mass at 7.2 meters. To prevent wrap-around of the neutrons, a thin ^{10}B enriched filter was placed in front of the ^6Li glass. Because of the ^{10}B cut-off, the efficiency was measured between 1 eV and 3 MeV. Since the neutron source had a
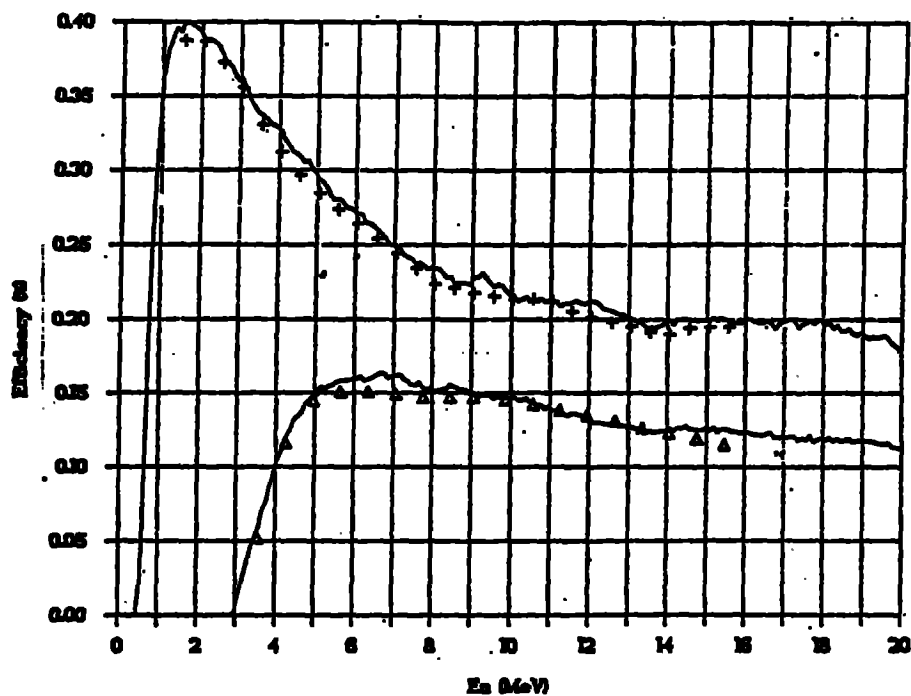
Fig. 2.   Calculated (solid lines) and measured
         efficiencies (crosses, triangles) for
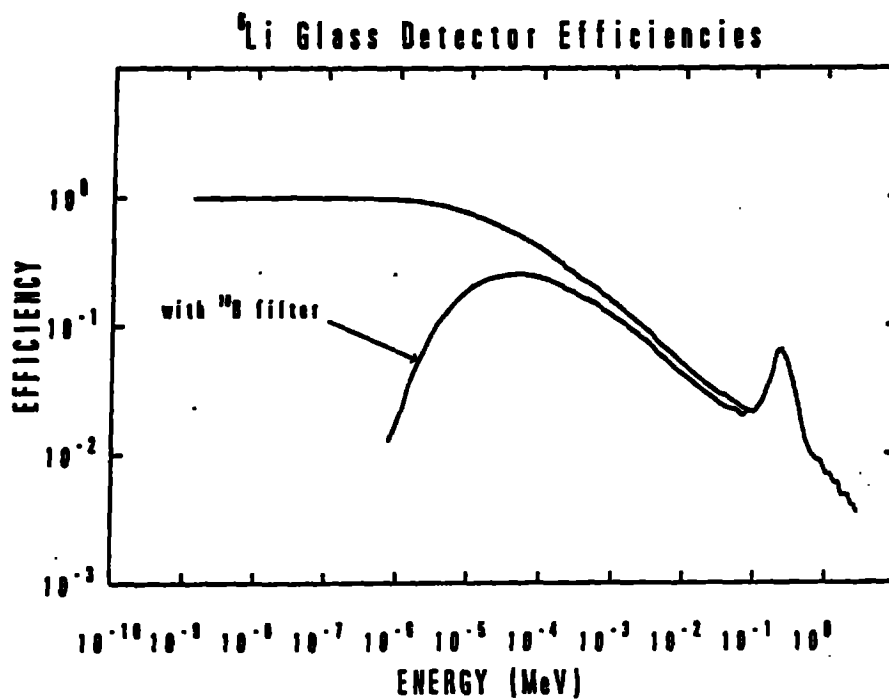   NE213 at two detector biases.

^{6}Li Glass Detector Efficiencies

Fig. 3 ^{6}Li glass detector efficiencies with
        and without the ^{10}B filter.

finite extent and the beam was tightly collimated in front of the fission chamber, a Monte-Carlo code was used to calculate the deviation from a $1/R^2$ behavior, thereby converting a relative shape measurement to an absolute efficiency determination. In addition, by bombarding a LiF target of known thickness with protons from the LLNL Tandem Van de Graaff, the absolute ^{6}Li glass efficiency was measured between 140 keV and 3 MeV. Between 140 keV and 3 MeV, there was good agreement between the absolute Tandem and Linac efficiency determinations. Between 100 keV and 1 eV, the shape of the calculated efficiency agrees well with that measured at the Linac; however, the calculated magnitudes were uniformly higher and agreement could be obtained by lowering the nominal ^{6}Li content by 17%. The efficiency with the ^{10}B filter is shown in Fig. 3 where the efficiency above 140 keV is obtained from the Linac and Tandem measurements and that between 1 eV and 140 keV is obtained from calculations with the nominal ^{6}Li content reduced by 17%. For measurements down to thermal energies the ^{10}B filter was removed, and the efficiency is shown in Fig. 3. The efficiency above 100 keV is identical to that with the ^{10}B filter while from thermal energy to 100 keV it is calculated, again with the nominal ^{6}Li content reduced by 17%. It should be mentioned that the efficiency with the 17% reduction in ^{6}Li content agrees with the measurements between 250 keV and ∿ 1 MeV. Above 1.5 MeV, the measured efficiency is lower than that calculated primarily because the pulse height window on the alpha plus triton recoils was set to reject events induced by ≥ 2 MeV neutrons. Because of the spread in pulse heights from the alpha plus triton recoils, the cut-off is not sharp and there is a measurable efficiency above 2 MeV and, at the same time, some recoils are also lost below 2 MeV neutron energy.

MEASUREMENTS

High Energy Emission Spectra

For the spectra measurements above 1 MeV, 5.1 cm diameter by 5.1 cm thick NE213 and Stilbene scintillators at two detector bias levels were used. Standard time-of-flight techniques with pulse shape discrimination to reject gammas were employed.[11] Fig. 4 shows the time-of-arrival spectra from the 3.5 MFP Be shell as measured with Stilbene for a ∿ 1 MeV detector bias. Clearly visible are the 14.8 MeV transmitted peak and the dip at 318 ns which is due to the Be resonance peak at 2.72 MeV. 500 ns time-of-arrival corresponds to a flight time of a 1.1 MeV neutron. Since the Stilbene measurements are very similar to those with NE213 and no additional information is obtained from the high bias measurements, only the NE213 low

bias results will be presented in Fig. 1 which shows the measured integrals of the spectra for various energy ranges for the three Be thicknesses.

Low Energy Emission Spectra

Measurements down to thermal energies were made using the ^{6}Li glass detector without the ^{10}B filter. The deuteron pulsing rate was 100 Hz and the burst width was 8 μs. Better resolution measurements were also made with a burst width of 250 ns and a deuteron pulsing rate of 1.67 kHz. To prevent neutron wrap-around at the higher repetition rate, the ^{10}B filter was reinserted. A 4096 channel Nuclear Data time digitizer in conjunction with a Nuclear Data Analyzer was used for data acquisition. In the buffer mode, the time digitizer could store 256 events per machine burst with a pulse pair resolution of 1 μs. Typical count rates at 100 Hz for the 3.5 MFP Be shell were ∿ 400 cts/sec or ∿ 4 counts per burst, resulting in negligible digitizer and analyzer dead times. For the better resolution measurements, the time per channel was a constant 125 ns. For the 100 Hz measurements the first 1024 channel had a 1 μs channel width which doubled for each subsequent 1024 channels. Since the maximum ramp time is 15 ms, the ramp was reset to zero at 9.9 ms, prior to the arrival of another start pulse (derived from the ion source arc pulsing) at 10 ms. No reset pulse was needed for the better resolution measurements as the maximum ramp time of 512 μs is shorter than the 600 μs pulsing period.

Four runs were taken to obtain the net counts from the Be. The Net Counts are given by:

$$\text{Net Counts} = (^6\text{Li} - k_1 {}^7\text{Li})_{\text{no absorber}}$$
$$- (k_2 {}^6\text{Li} - k_3 {}^7\text{Li})_{{}^6\text{LiD absorber}}$$

where ^{7}Li is a run taken with an identical scintillator containing enriched ^{7}Li. The constants k_1, k_2 and k_3 are used to normalize the neutron production for the respective runs as measured by the alpha counts to that recorded for the ^{6}Li no absorber run. The thick ^{6}LiD absorber was spherical and the transmission was less than 0.5% for neutrons ≤ 3 MeV.

The no absorber subtraction yields counts from all neutrons reaching the detector while the ^{6}LiD absorber subtraction yields counts from inscattered background neutrons, i.e. those neutrons not directly emanating from the Be. For the 3.5 MFP Be shell at 100 Hz pulsing rate, the total counts in the spectrum from inscattered neutrons is 0.25% of the

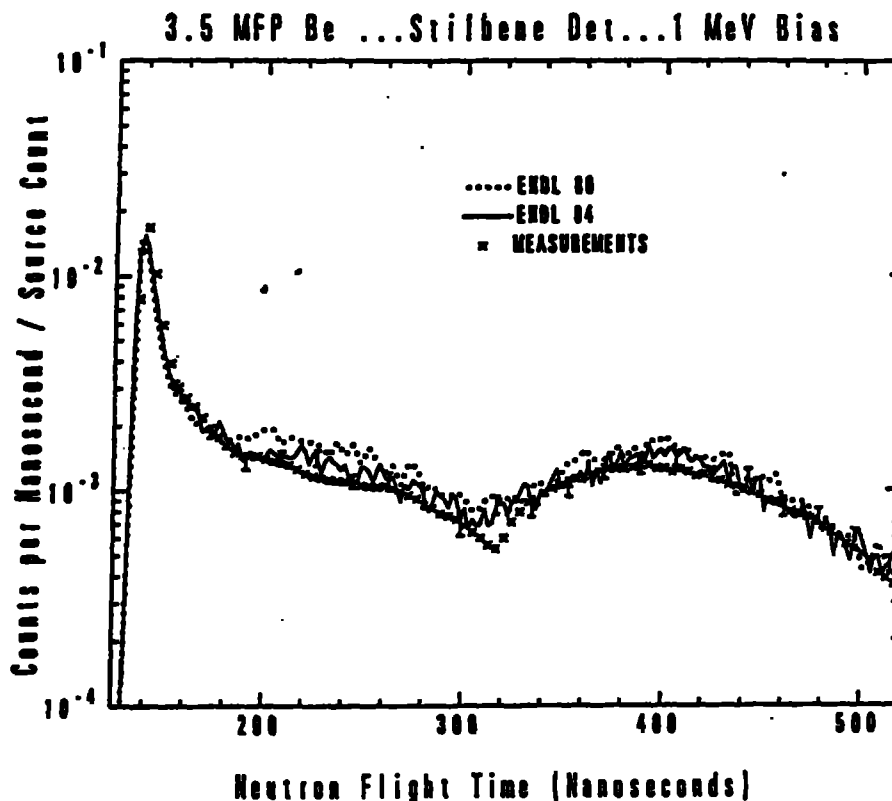## 3.5 MFP Be ...Stilbene Det...1 MeV Bias

Fig. 4   Measured and calculated high energy
time-of-arrival spectra for 3.5 MFP Be
at 1 MeV Stilbene detector bias.

counts from neutrons coming directly from the Be; the corresponding number for the 2.5 MFP Be is 2%. Consequently, in a later measurement to check reproducibility, ^{6}LiD absorber runs were not taken. Additional checks were made by inserting 0.05 cm thick cadmium and 0.013 cm thick gold absorbers between the helium bags. In the case of cadmium, all neutrons below ∿ .3 eV were removed; with gold a resonance dip was observed at a flight time of 237 μs, in good agreement with the energy of the gold resonance at 4.9 eV. As expected, the resonance dip for 3.5 MFP Be is shallow (factor of 9 reduction) and broad (∿ 21 μs FWHM, or 0.85 eV wide), showing that there is less than a perfect correlation between time-of-arrival and energy. Figs. 5,6 show the measured time-of-arrival spectra for the 2.5 and 3.5 MFP Be shells. The energies indicated by the arrows are calculated assuming a point source and a 7.28 m flight path. As such they should be regarded as approximate indications of the actual energies involved.

MONTE CARLO CALCULATIONS

Monte Carlo calculations were performed with the Alice neutron transport code (14). The target assembly, source description (15), and Be geometry were modeled exactly. The helium was incorporated as spherical shells alternating with shells of air. The tally zone was a spherical annulus at 7.28 m extending from 0 = 11° to 35°. For each neutron entering the tally zone, its time-of-arrival, energy, and directional cosines with respect to the normal are tabulated. The Alice output is then edited by folding in the detector efficiency which is a function of neutron energy and requiring that the angle with the normal is smaller than the angle for neutrons coming directly from the shell. Finally, the experimental burst widths, as mentioned earlier, were folded into the calculations with a Gaussian time resolution function. The calculated time-of-arrival spectra are shown in Figs. 4, 5 and 6.
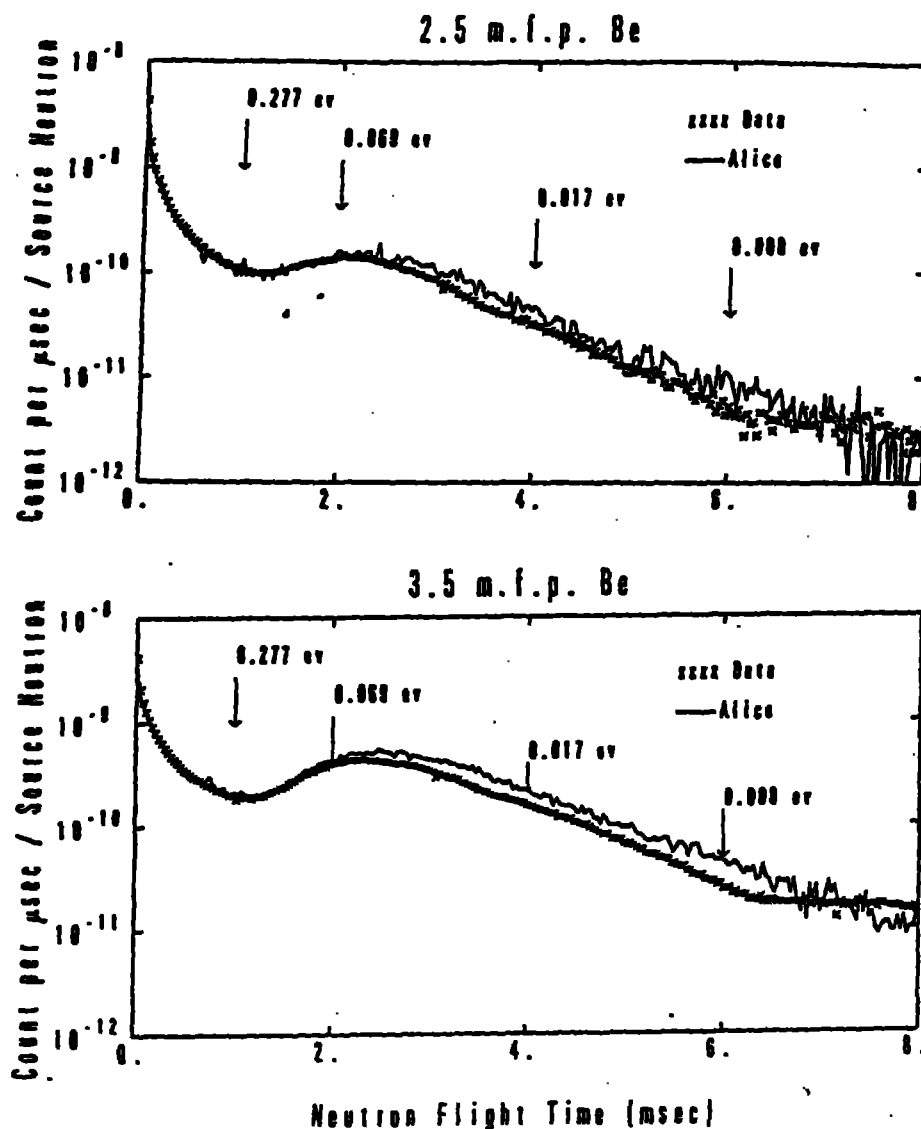
Fig. 5   Measured and calculated low energy
          time-of-arrival spectra out to 8 ms for
          2.5 and 3.5 MFP Be.

The leakage multiplications calculated using ENDL-84 are 1.64 for the 2.5 MFP and 1.89 for the 3.5 MFP Be assemblies. Without the missing hemispherical shells, the corresponding calculated leakage multiplications are increased to 1.87 and 2.02, respectively.

DISCUSSION

From Fig. 4 it is evident that ENDL-84 does better than ENDL-80 in fitting the high energy spectra measurements. From Fig. 4 and Table I it is also clear that ENDL-84 underestimates the spectra above 10 MeV and overestimates the spectra between 2 and 10 MeV.

Figs. 5 and 6 show the low energy spectra for 2.5 and 3.5 MFP Be measured at 100 Hz and 8 µs pulse width. Fig. 6 is an expanded plot showing the spectra for the first 1 ms. Clearly evident from Fig. 6 is the underestimation of the spectra by ENDL-84 from ∼ 2 MeV down to 28 eV (100 µs) for the 3.5 MFP Be and down to 7 eV (200 µs) for the 2.5 MFP Be. This underestimation has been verified quantitatively using the better resolution measurement at 1.667 kHz and 250 ns burst width. It is also evident from Fig. 5 that ENDL-84 overestimates the epithermal and thermal flux with the discrepancy being larger for the 3.5 MFP Be.
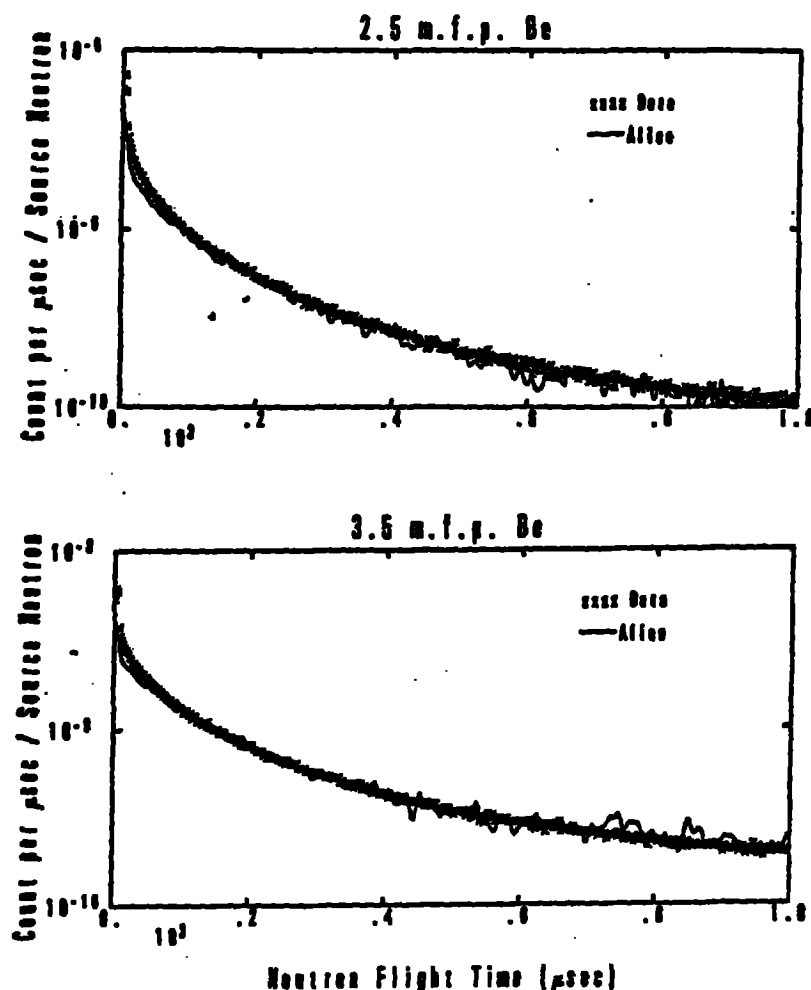
Fig. 6   Measured and calculated low-energy
time-of-arrival spectra out to 1 ms for
2.5 and 3.5 MFP Be.

CONCLUSIONS

ENDL-84 predicts that 30% of the leakage
neutrons are below 28 eV for the 3.5 MFP Be.
Fig. 5 shows that this predicted copious
emission of thermal and epithermal neutrons
has been verified. The average number of
collisions experienced by a neutron before
escaping the 3.5 MFP Be shell is 94. The good
agreement in the shape of the measured and
calculated spectra in Figs. 5 and 6 thus
provides an excellent validation of the
correctness of the Alice Monte Carlo neutron
transport code.

Table I and Fig. 4 show that ENDL-84
underestimates the spectra above 10 MeV and
overestimates the spectra between 2 and 10

MeV. Fig. 5 shows that ENDL-84 overestimates
the spectra in the epithermal and thermal
regions while Fig. 6 shows that it
underestimates the leakage spectra between 28
eV and ∿ 2 MeV. Weighting the measured
discrepancies with the calculated fractional
population of neutrons in each region (see
Table II) , the deduced measured leakage
multiplication is ∿ 3% higher than ENDL-84
calculations for the 3.5 MFP Be and ∿ 9%
higher in the case of the 2.5 MFP Be.
Considering the uncertainties in the
efficiencies and in the method for deducing
the leakage multiplication, it is estimated
that the inferred measured leakage
multiplications are accurate to ± 10%. A
more detailed analysis now in progress will
quantify this uncertainty more precisely.

Table I. Measured and Calculated Integrals (counts/source count) for NE213 at
1 MeV Detector Bias using ENDL-84

Shell Thickness	E>10MeV	5<E<10	1<E<5	Total
0.8 MFP				
Calc.	.724	.118	.321	1.163
Exp.	.743	.114	.312	1.169
Ratio	.974	1.035	1.029	.995
2.5 MFP				
Calc.	.350	.134	.386	.870
Exp.	.373	.127	.372	.872
Ratio	.938	1.055	1.038	.998
3.5 MFP				
Calc.	.207	.114	.337	.658
Exp.	.225	.106	.322	.653
Ratio	.920	1.076	1.047	1.008

Table II. Fractional Neutron Population and Ratio of Calculated
to Measured Integrals of the Leakage Spectra for 2.5
and 3.5 MFP Be.

	2.5 MFP Be		3.5 MFP Be	
ΔE	$\frac{\text{Calc (ENDL-84)}}{\text{Meas.}}$	Neutron Population (ENDL-84)	$\frac{\text{Calc(ENDL-84)}}{\text{Meas.}}$	Neutron Population (ENDL-84)
15MeV-10MeV	0.938	0.307	0.92	0.159
10MeV-2MeV	1.055	0.227	1.076	0.185
2MeV-2.8keV	0.697	0.282	0.698	0.249
2.8keV-0.77eV	0.919	0.120	0.956	0.169
0.77eV-0.28eV	0.949	0.003	1.073	0.016
0.28eV-0.03eV	1.097	0.055	1.15	0.174
0.03eV-0.006eV	1.36	0.006	1.41	0.048
	D_i	P_i	D_i	P_i

$$D = \sum_i D_i \, P_i$$

D = 0.91   D = 0.97

References

(1) J. D. LEE, "Nucleonics of a Be-Li-Th Blanket for the Fusion Breeder," Nucl. Technol./Fusion, 4, 805 (1983).

(2) Blanket Comparison and Selection Study (BCSS), to be published.

3) P. CLOTH, D. FILGES, R. HERZING, and M. KIRCH, "Neutron Multiplication effect of CTR Blankets Containing Beryllium," Proc. 9th Symp. Fusion Technology, Garmisch-Partenkirchen, FRG, Pergamon Press (1976).

(4) T. K. BASU, V. R. NARGUNDKAR, P. CLOTH, D. FILGES, and S. TACZANOWSKI, "Neutron Multiplication Studies in Beryllium for Fusion Reactor Blankets," Nucl. Sci. Eng., 70, 309 (1979).

(5) T. K. BASU, "Studies on Multiplication of 14-MeV Neutrons in Beryllium Assemblies for Fusion Reactor Blankets," Ph.D. Thesis, University of Bombay (1980).

(6) V. R. NARGUNDKAR, T. K. BASU and O. P. JONEJA, "Re-Analysis of Neutron Multiplication Measurements in Thick Beryllium and Graphite Assemblies for 14 MeV Neutrons", submitted to Fusion Technology (Aug. 11, 1984).

(7) V. R. NARGUNDKAR, T. K. BASU, O. P. JONEJA, M. R. PHISKI and S. K. SADAVARTE, "Neutron Multiplication Measurement in BeO for 14-MeV Neutrons," Fusion Technology, 6, 93 (1984).

(8) S. T. PERKINS, "A Calculation of the Angular and Energy Distributions for Neutrons from the $^9Be(n,2n)$ Reaction," UCRL-50520, Lawrence Livermore National Laboratory, (1968).

(9) R. J. HOWERTON, R. E. DYE and S. T. PERKINS, "Evaluated Nuclear Data Library," UCRL-50400, Lawrence Livermore National Laboratory, Livermore, CA, Vol. 4, Rev. 1 (1981)

(10) S. T. PERKINS, E. F. PLECHATY and R. J. HOWERTON, "A reevaluation of the $^9Be(n,2n)$ Reaction and Its Effect in Neutron Multiplication in Fusion Blanket Applications," UCRL-91276, Lawrence Livermore National Laboratory, (1984), (submitted to Nuclear Science and Engineering).

(11) C. WONG, J. D. ANDERSON, P. BROWN, L. F. HANSEN, J. L. KAMMERDIENER, C. LOGAN, and B. A POHL, "Livermore Pulsed Sphere Program: Program Summary Through July 1971," UCRL-51144, Rev. I, Lawrence Livermore National Laboratory (1972).

(12) H. H. BARSCHALL, R. BOOTH and C. WONG, "Neutron flux Measurement at RTNS Facility", UCID-17206, Lawrence Livermore National Laboratory (1976).

(13) G. DIETZE and H. KLEIN, Physikalisch-Technische Bundesanstalt, Braunschweig, PTB-ND-22 (October 1982).

(14) E. F. PLECHATY and J. R. KIMLINGER, "TARTNP: A coupled neutron-photon Monte Carlo transport code", UCRL-50400 Vol. 14, Lawrence Livermore National Laboratory (1976).

(15) J. D. SEAGRAVE, "The $D(d,n)He^3$ and $T(d,n)He^4$ Neutron Source Handbook", LAMS 2162, Los Alamos National Laboratory(1958).